

# MECHANICAL BEHAVIOR AND MICROSTRUCTURE EVOLUTION OF THE Ti-3Al-5Mo-4.5V ALLOY AT AN ELEVATED DEFORMATION TEMPERATURE

## MEHANSKE LASTNOSTI IN RAZVOJ MIKROSTRUKTURE ZLITINE Ti-3Al-5Mo-4,5V PRI POVIŠANIH TEMPERATURAH DEFORMACIJE

Menglan Shen<sup>1</sup>, Yuanming Huo<sup>1\*</sup>, Tao He<sup>1</sup>, Yong Xue<sup>2</sup>, Yujia Hu<sup>1</sup>, Wanbo Yang<sup>1</sup>

<sup>1</sup>School of Mechanical and Automotive Engineering, Shanghai University of Engineering Science, Shanghai 201620, China.  
<sup>2</sup>School of Material Science and Engineering, North University of China, Taiyuan 030051, China.

*Prejem rokopisa – received: 2020-05-25; sprejem za objavo – accepted for publication: 2021-02-24*

doi:10.17222/mit.2020.088

A high-performance titanium alloy requires a fine and homogenous microstructure. The rational deformation process parameters of the Ti-3Al-5Mo-4.5V (TC16) titanium alloy can contribute to achieving this important microstructure. Hot-compression experiments were performed at temperatures in the range 100–800 °C and at strain rates of 0.1 s<sup>-1</sup> to 10.0 s<sup>-1</sup>. The effects of deformation temperatures and deformation rates on the mechanical behaviour and microstructure evolution were analysed and discussed. The softening mechanism of the Ti-3Al-5Mo-4.5V alloy at an elevated deformation temperature was revealed. Experimental results showed that 500 °C is the critical deformation temperature to distinguish the warm-deformation region of 100–400 °C and the hot-deformation region of 500–800 °C. The softening mechanism is dominated by  $\beta$ -phase spheroidization in the temperature range 100–400 °C with a higher strain rate of 10.0 s<sup>-1</sup>. The softening mechanism is dominated by a local temperature rise in the temperature range 500–800 °C with a lower strain rate of 0.1 s<sup>-1</sup>.

Keywords: isothermal compression, mechanical behavior, microstructure evolution, softening mechanism

Za visoko kvalitetne Ti zlitine je značilna oziroma se zahteva drobnozrnata in homogena mikrostruktura. K doseganju takšne mikrostrukture lahko pripomorejo ustrezni parametri deformacije izbrane Ti zlitine tipa Ti-3Al-5Mo-4.5V (TC16). Avtorji v članku opisujejo preizkuse vroče tlačne deformacije v temperaturnem območju med 100 °C in 800 °C pri hitrostih deformacije med 0,1 s<sup>-1</sup> in 10,0 s<sup>-1</sup>. Analizirali in ugotavljali so vpliv temperature in hitrosti deformacije na mehansko obnašanje in razvoj mikrostrukture izbrane zlitine. Odkrili so, da je pri povišanih temperaturah in hitrostih deformacije prišlo do mehanizma mehčanja izbrane Ti-3Al-5Mo-4.5V zlitine. Eksperimentalni rezultati so pokazali, da je 500 °C kritična temperatura deformacije, od katere naprej (500 °C do 800 °C) se deformacijski mehanizmi razlikujejo od tistih v temperaturnem območju med 100 °C in 400 °C. Za mehanizem mehčanja je odločilna sferoidizacija faza  $\beta$  v temperaturnem območju med 100 °C in 400 °C in najvišji hitrosti deformacije 10,0 s<sup>-1</sup>. Za prevladujoč mehanizem mehčanja v temperaturnem območju med 500 °C in 800 °C pa so značilne najnižje hitrosti deformacije 0,1 s<sup>-1</sup>.

Ključne besede: izotermično stiskanje, mehansko obnašanje, razvoj mikrostrukture, mehanizem mehčanja

## 1 INTRODUCTION

For several decades, titanium and its alloys have been used to manufacture structural parts in aeronautics and astronautics owing to their excellent mechanical properties, such as high specific strength and excellent resistance to high temperature.<sup>1</sup> Two kinds of titanium alloy material, Ti-6Al-4V and Ti-3Al-5Mo-4.5V, were often used to manufacture aerospace fasteners. The Ti-6Al-4V alloy was first developed by the USA in 1954. It is a martensitic  $\alpha + \beta$  two-phase middle-strength titanium alloy and can be worked at 400 °C for a long time. However, hot forming is the only way for TC4 to manufacture fasteners owing to its poor cold plasticity.<sup>2</sup> Compared with the Ti-6Al-4V alloy, Ti-3Al-5Mo-4.5V can be used to produce the aerospace fasteners by cold forging due to its good plastic-deformation capacity at room tempera-

ture. It is a martensitic  $\alpha + \beta$  two-phase high-strength titanium alloy.<sup>3</sup> Therefore, Ti-3Al-5Mo-4.5V became popular for the forming of aerospace fasteners all over the world.

Some publications about Ti-3Al-5Mo-4.5V have been found. Wang et al. investigated the microstructure evolution in adiabatic shear band in a fine-grain-sized Ti-3Al-5Mo-4.5V alloy, and the results showed that the fine, equiaxed grains with  $\alpha$  phase and  $\alpha'$  phase coexist in the shear band.<sup>4</sup> Li et al. studied the tensile deformation behavior of the Ti-3Al-5Mo-4.5V titanium alloy, they found that there are obvious yield points on the true stress-strain curves of annealing structures, then a stress drop occurs.<sup>5</sup> Wu discussed the effects of heat upsetting on the microstructure and properties of the Ti-3Al-5Mo-4.5V alloy, and found that the proper heat upsetting temperature is 700 °C for the Ti-3Al-5Mo-4.5V alloy. When the heat upsetting temperature is too high, a local temperature rise will occur.<sup>6</sup> Song et al. studied the ef-

\*Corresponding author's e-mail:  
yuanming.huo@sues.edu.cn (Yuanming Huo)

fects of microstructural change on the dynamic compressive deformation behavior of the Ti-3Al-5Mo-5V alloy. The results showed that the microstructure characteristics, such as the length, width and the aspect ratio of the  $\alpha$  platelets, changes regularly with the increase of temperature or holding time. The aspect ratio and the size of the  $\alpha$  platelet affect the width of the deformed shear band forming during the dynamic compressive deformation.<sup>7</sup> Gao et al. analyzed the microstructure evolution of a Ti-3Al-5Mo-5V alloy bar during hot working, and obtained finer structure grains and better structure homogeneity by means of controlling the deformation parameter.<sup>8</sup> Shen et al. built constitutive equations of the Ti-3Al-5Mo-4.5V alloy by using a double multiple non-linear regression model and a strain-compensated Arrhenius model, and compared the difference between the two different models at the elevated deformation temperature.<sup>9</sup> The above research is involved in all aspects of Ti-3Al-5Mo-5V alloy. However, mechanical behavior and microstructure evolution of Ti-3Al-5Mo-4.5V alloy at the high, elevated deformation temperatures range from 100–800 °C has been seldom published. Especially, there is a lack of studies of the effects of deformation temperatures and deformation rates on the mechanical behavior and the microstructure evolution.

The aim of this work was to study the deformation behaviour and microstructure evolution of the Ti-3Al-5Mo-4.5V alloy at an elevated temperature. Firstly, hot-compression tests were conducted with different process parameters to measure the stress-strain relationship of the Ti-3Al-5Mo-4.5V alloy. Secondly, we sectioned the compressed specimens and polished them for investigating their microstructures. Thirdly, the effects of deformation temperatures and deformation rates on the mechanical behavior and microstructure evolution were discussed. The deformation softening mechanism of Ti-3Al-5Mo-4.5V was analyzed.

## 2 EXPERIMENTAL PROCEDURES

A cylinder with a diameter of 8 mm and height of 12 mm was machined from a wire rod using a wire-cutting machine to prepare specimens. The original microstructure of the ingot was captured by scanning electron microscope (SEM), shown in **Figure 1**. It is composed of a basket-weave microstructure, including the  $\alpha$  phase and  $\beta$  phase. The black equiaxed and stripe phase is the  $\alpha$  phase. Zhrebtsov et al. defined the aspect ratio of the equiaxed  $\alpha$  phase to be,  $k = l / b < 2$ , where  $l$  and  $b$  are the length and thickness, respectively, of the  $\alpha$  phase.<sup>10</sup> The microstructural parameters were measured manually based on ASTM: E 112-12. For a constituent phase, the grain boundaries were picked up manually. The length of the  $\alpha$  phase is about 1.5  $\mu\text{m}$ , and the thickness of the  $\alpha$  phase is about 0.8  $\mu\text{m}$ . The  $\alpha$  phase and  $\beta$  phase are both evenly distributed in the alloy.

The experimental procedures were carried out in a Gleeble 3800 thermal mechanical simulator. The  $\beta$ -phase transition temperature (at which  $\alpha + \beta \rightarrow \beta$ ) of the Ti-3Al-5Mo-4.5V alloy was approximately 865 °C.<sup>11</sup> The deformation temperatures in this work were selected in the range 100–800 °C. The detailed hot-compression process was shown in **Figure 2**. Firstly, the specimens were respectively heated to the deformation temperature (100 °C, 200 °C, 300 °C, 400 °C, 500 °C, 600 °C, 700 °C, 800 °C) with a rate of 5 °C/s. Then, the specimens were held for 3 min at the individual deformation temperature for temperature uniformity. Subsequently, the specimens were compressed to a true strain of 1.0 with a strain rate of 0.1  $\text{s}^{-1}$ , 1.0  $\text{s}^{-1}$  and 10.0  $\text{s}^{-1}$ . The deformed specimens were quenched with water to freeze the microstructure. True stress-strain relationships were measured during hot compression.

It is vital to investigate the microstructure of compressed specimens. The compressed specimens were sectioned along the longitudinal direction. The sectioned surfaces were grinded with a waterproof abrasive paper, and polished to a mirror surface with a polishing ma-

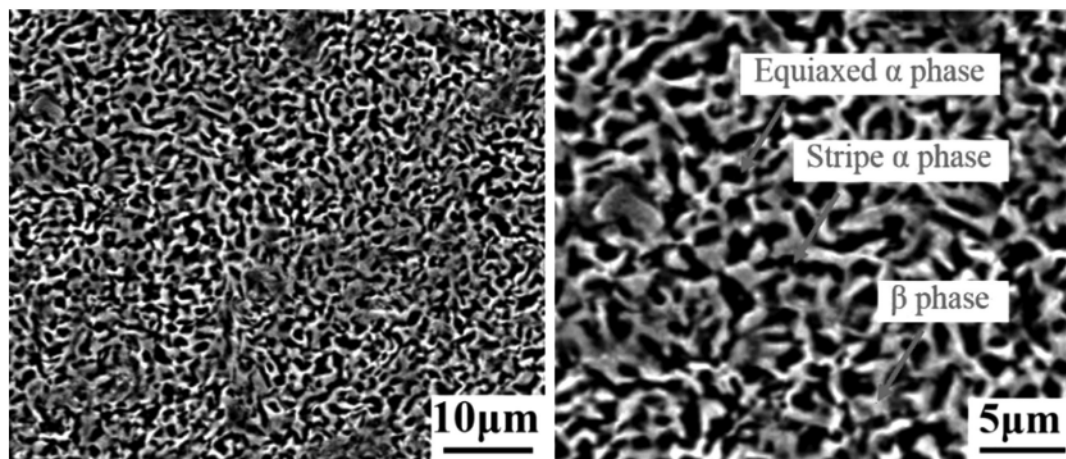


**Figure 1:** Initial SEM micrographs of Ti-3Al-5Mo-4.5V alloy

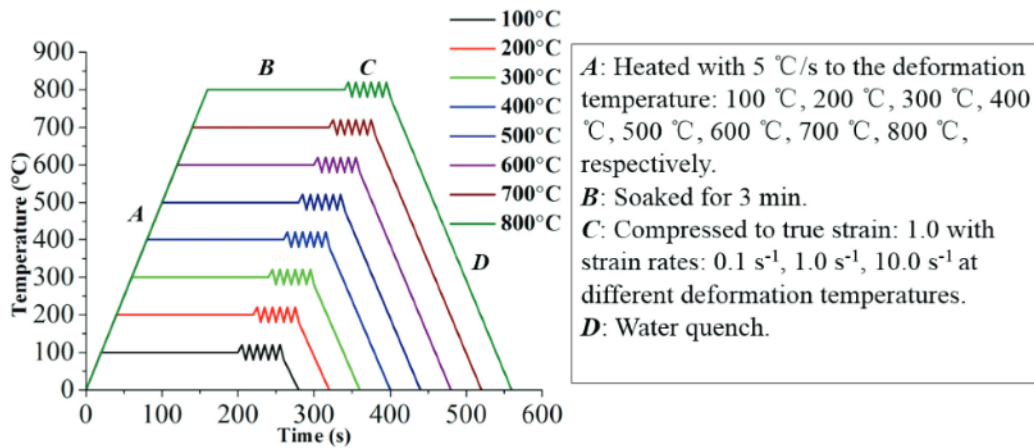


Figure 2: Schematic depiction of hot-compression process.

chine. And then, the polished surfaces need to be etched using mixed acid solution, which consists of 2.5 mL HF, 3 mL HNO<sub>3</sub>, 5 mL HCl and 91 mL H<sub>2</sub>O. The microstructure distribution was revealed after acid corrosion. The micrographs were captured using the SEM.

### 3 EXPERIMENTAL RESULTS AND DISCUSSIONS

#### 3.1 Effect of deformation temperatures on the mechanical behavior

Figure 3 shows the stress-strain relationships of Ti-3Al-5Mo-4.5V at temperatures of 100 °C, 200 °C, 300 °C, 400 °C, 500 °C, 600 °C, 700 °C and 800 °C with strain rates of 0.1 s<sup>-1</sup>, 1.0 s<sup>-1</sup> and 10.0 s<sup>-1</sup>. Relative softening (RS) rate was used to quantitatively describe the extent of the dynamic softening of the Ti-3Al-5Mo-4.5V. The RS can be calculated as follows by using the relationship between  $\sigma_p$  and  $\sigma_i$ .<sup>12</sup>

$$RS = \frac{\sigma - \sigma_i}{\sigma_p} \quad (1)$$

In Equation 1,  $\sigma_p$  and  $\sigma_i$  are the peak flow stress and flow stress at the strain of 0.8, respectively. If  $RS > 0$ , it indicates that dynamic softening takes advantage,  $RS = 0$  means that work hardening and metal softening reached a balance, and  $RS < 0$  indicates that work hardening takes advantage. Figure 4 shows the RS rate under dif-

ferent deformation conditions. It can be seen from Figure 3 that the critical deformation temperature is 500 °C. At 500 °C, the flow stress of the Ti-3Al-5Mo-4.5V alloy almost remains stable. This is because the work hardening and metal softening reached a balance, as Figure 4 shows that the RS of each strain rate at 500 °C nearly equalled zero.

For the same strain rate of 0.1 s<sup>-1</sup>, when the deformation temperature is lower than 500 °C, the value of true stress increases with the increase of the plastic strain. The values of RS in this situation are negative, as Figure 4 shows. That is to say the work hardening is predominant during the metal forming when the deformation temperature is lower than 500 °C. When plastic deformation occurs, the strength of titanium alloys will increase, and more external forces must be applied to metal materials. For the same strain rate of 0.1 s<sup>-1</sup>, when the deformation temperature is higher than 500 °C, the values of RS in this situation are positive, as Figure 4 shows. The softening mechanism predominates during hot compression, whose stress value decreases with the increase of the plastic strain. Ding et al. thought that the phase transition, adiabatic temperature rise, dynamic recovery and dynamic recrystallization may happen, which caused the material softening.<sup>13</sup> Local temperature rise here is regarded as the main reason for material softening, which will be discussed in detail in the following.

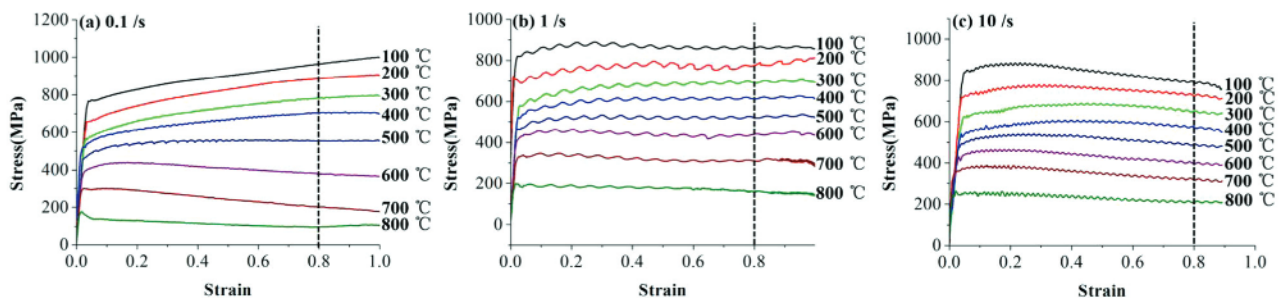


Figure 3: Stress-strain relationships of Ti-3Al-5Mo-4.5V at strain rates of: a) 0.1 s<sup>-1</sup>, b) 1.0 s<sup>-1</sup> and c) 10.0 s<sup>-1</sup>

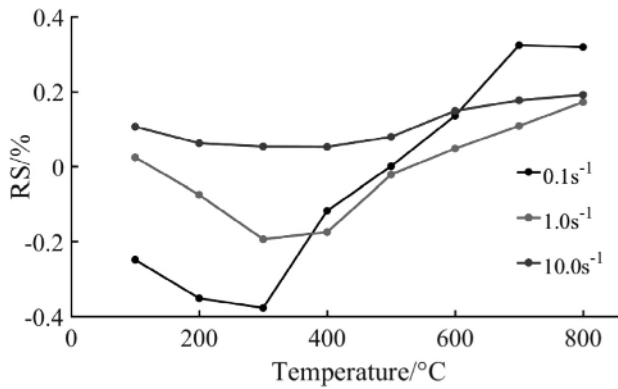


Figure 4: RS rate under different hot compression conditions

The higher deformation temperature leads to a higher dynamic softening at the lower strain rate of 0.1 s<sup>-1</sup>.

However, the case is different at the higher strain rate of 10.0 s<sup>-1</sup>. The dynamic softening is obvious in the temperature range 100–400 °C with the higher strain rate of 10.0 s<sup>-1</sup>. This softening mechanism may be controlled by microstructure spheroidization in the alloy, which will be discussed in Section of 3.2.

For the same deformation temperature, the oscillation frequency of stress-strain curve increases with the increase of the strain rate. When the strain rate is 0.1 s<sup>-1</sup>, it is hard to see an oscillation in Figure 3a. The oscillation frequency of the stress-strain curve is very high at the strain rate of 10.0 s<sup>-1</sup>. It indicates that the competition between the work hardening and dynamic softening is fierce during hot compression at a higher strain rate of 10.0 s<sup>-1</sup>. The formation of a large number of new movable dislocations at grain and grain boundaries is the fundamental reason for the sharp increase of flow stress. This new movable dislocation will also accumulate in the process of deformation and produce a new stress concentration. When the stress concentration reaches a certain degree, the microstructure evolution caused by it will reduce the movable dislocation density. The new production and old annihilate of movable dislocation thus causes the phenomenon of stress oscillation at the higher strain rate.<sup>14</sup> A higher strain rate can accelerate this dislocation evolution mechanism, so the oscillation frequency of the stress-strain curve is very high at a higher strain rate of 10.0 s<sup>-1</sup>. Luo thought that the continuous oscillation of flow stress may be due to unstable deformation, but has nothing to do with the softening mechanisms of the material.<sup>15</sup>

According to Figure 3, most flow stresses tend to be stable at the strain of 0.8. So, we calculated that the stress value decreases by 95 MPa and 84 MPa, respectively, for each increase of 100 °C at the strain of 0.8 with the strain rate of 1.0 s<sup>-1</sup> and 10.0 s<sup>-1</sup>. When the strain rate is 0.1 s<sup>-1</sup>, for each increase of 100 °C, the stress value decreases about 126 MPa at the strain of 0.8. It indicates that the decrease of the stress value is reduced with the increase of strain rate for each increase of

100 °C. That is to say that higher strain rate will reduce the material softening effect during deformation.

### 3.2 Effect of deformation temperatures on the microstructure evolution

Figure 5 shows the SEM micrographs of Ti-3Al-5Mo-4.5V under a strain rate of 10.0 s<sup>-1</sup> and a strain of 1.0 at deformation temperatures of 100 °C, 200 °C, 300 °C and 400 °C. The compression deformation direction (CD) and radial direction (RD) of specimens were indicated in Figure 5. It can be seen from Figure 5 that the amount of the spheroidized β phase increases with the increase of the deformation temperature. This is because the higher deformation temperature provides sufficient thermal driving force and stacking energy for the β phase to complete the spheroidization process. So, with the spheroidization of the β phase, the true stress-strain curve shows a softening trend. Spheroidization of the β phase is obvious in Figure 5a, which corresponds to the flow stress decreases as the increased of the plastic strain under a strain rate of 10.0 s<sup>-1</sup> at 100 °C, in Figure 3c.

When the temperature is 400 °C, the distribution of the α phase and the spheroidized β phase is very uniform, no coarse grain appears in this situation. By observing the corresponding stress-strain curves in Figure 3c, it can be found that after the elastic stage, the flow stress tends to be stable; and the peak flow stress is about 580 MPa. Therefore, this deformation temperature is conducive to the material processing of Ti-3Al-5Mo-4.5V.

Figure 6 shows the SEM micrographs of the Ti-3Al-5Mo-4.5V under a strain rate of 10.0 s<sup>-1</sup> and strain of 1.0 at deformation temperatures of 500 °C, 600 °C, 700 °C and 800 °C. When the temperature is 500 °C, the phenomenon of β-phase coarsening is obvi-

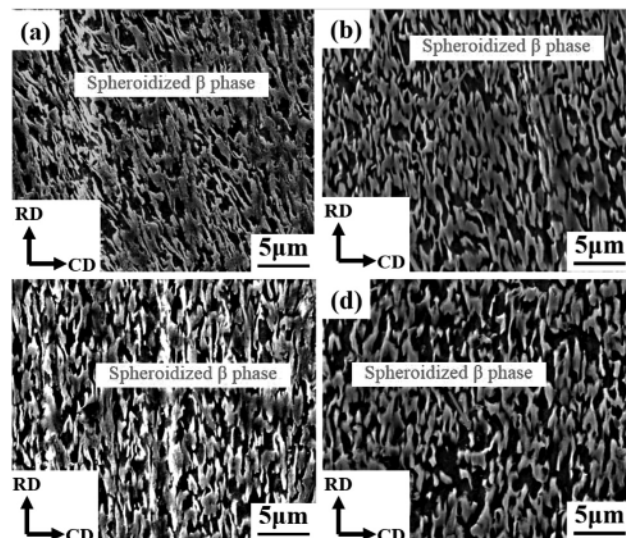


Figure 5: SEM micrographs of Ti-3Al-5Mo-4.5V under a strain rate of 10.0 s<sup>-1</sup> and strain of 1.0 at different temperatures of: a) 100 °C, b) 200 °C, c) 300 °C and d) 400 °C

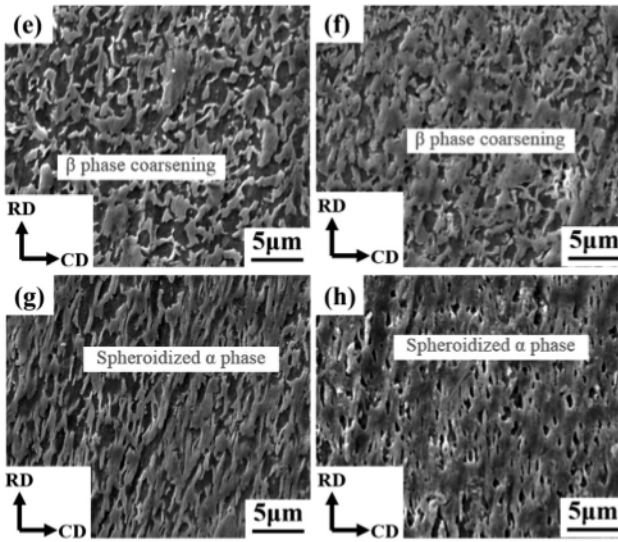


Figure 6: SEM micrographs of Ti-3Al-5Mo-4.5V under a strain rate of  $10.0 \text{ s}^{-1}$  and strain of 1.0 at different temperatures: e)  $500 \text{ }^\circ\text{C}$ , f)  $600 \text{ }^\circ\text{C}$ , g)  $700 \text{ }^\circ\text{C}$  and h)  $800 \text{ }^\circ\text{C}$

ous. And the average size of the  $\alpha$  phase is smaller when the temperature is  $600 \text{ }^\circ\text{C}$ . It shows that a small amount of  $\alpha$  phase started to transform into  $\beta$  phase. Chongzhou holds a view that the severe deformation produces latent heat, which stimulates the local temperature rise of the titanium alloy. And the increase of the local temperature made a small amount of  $\alpha$  phase reach the phase-transition temperature.<sup>6</sup>

When the temperature is  $700 \text{ }^\circ\text{C}$  and  $800 \text{ }^\circ\text{C}$ , more and more  $\alpha$  phase transformed into  $\beta$  phase. The globularization of the  $\alpha$  phase started at  $700 \text{ }^\circ\text{C}$ , Li thought that the globularization started to occur in the middle part of the partial  $\alpha$  phase, and the  $\alpha$  phase in the middle part transforming to  $\beta$  phase caused the  $\alpha$  phase's disconnection during compression. The disconnected  $\alpha$  phase was transformed into spheroidized  $\alpha$  phase.<sup>16</sup> At  $800 \text{ }^\circ\text{C}$ , the  $\alpha$  phase is almost completely spheroidized. The spheroidization of the  $\alpha$  phase is a thermal activation process.<sup>17</sup>

From above analysis, at the strain rate of  $10.0 \text{ s}^{-1}$ ,  $\beta$ -phase spheroidization is obvious in the temperature range  $100\text{--}400 \text{ }^\circ\text{C}$ . The phase transition of  $\alpha$  phase is obvious in the temperature range  $700\text{--}800 \text{ }^\circ\text{C}$ . The results indicate that the softening mechanism is controlled by microstructure spheroidization under the higher strain rate at the temperature range  $100\text{--}400 \text{ }^\circ\text{C}$ . This is consistent with the assumption in Section 3.1. For the same strain rate, a deformation temperature of  $400 \text{ }^\circ\text{C}$  is beneficial for manufacturing Ti-3Al-5Mo-4.5V with good mechanical properties and uniform microstructure.

### 3.3 Effect of deformation rates on the mechanical behavior

Figure 7 shows the stress-strain relationships of Ti-3Al-5Mo-4.5V at strain rates of  $(0.1, 1.0 \text{ and } 10.0) \text{ s}^{-1}$  with deformation temperatures of  $100 \text{ }^\circ\text{C}$ ,  $200 \text{ }^\circ\text{C}$ ,

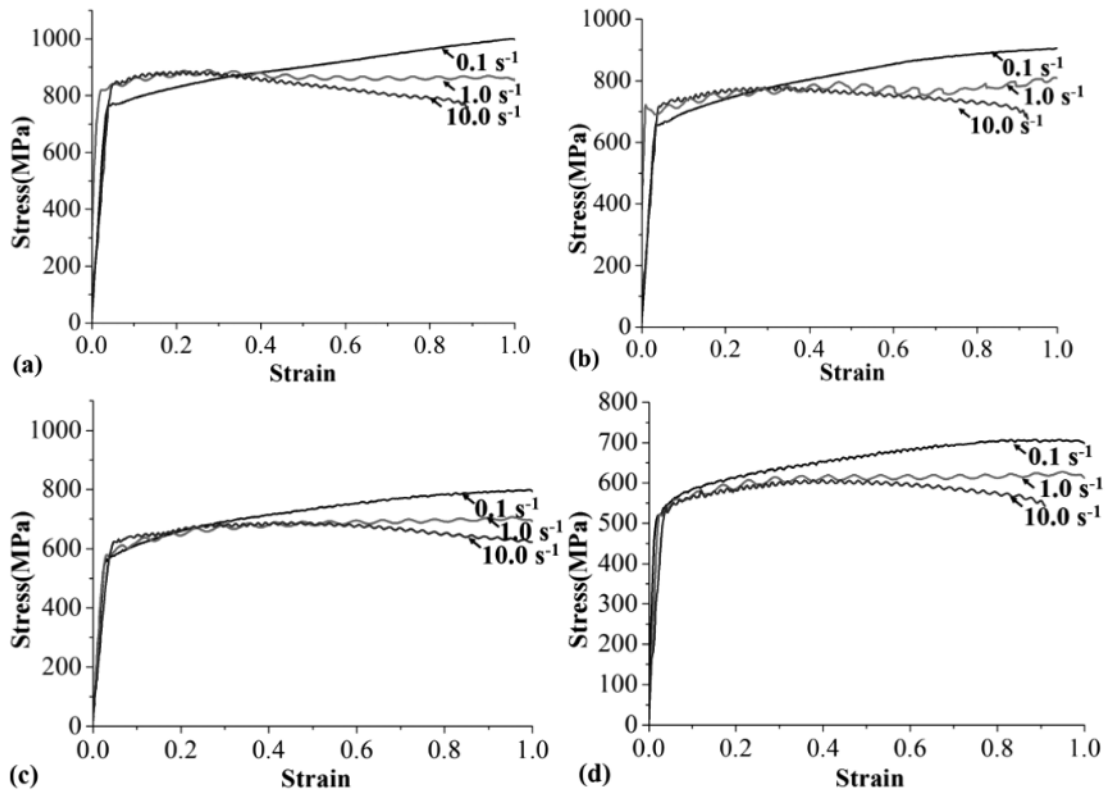


Figure 7: Stress-strain relationships of Ti-3Al-5Mo-4.5V at strain rates of  $0.1 \text{ s}^{-1}$ ,  $1.0 \text{ s}^{-1}$  and  $10.0 \text{ s}^{-1}$  with temperatures of: a)  $100 \text{ }^\circ\text{C}$ , b)  $200 \text{ }^\circ\text{C}$ , c)  $300 \text{ }^\circ\text{C}$  and d)  $400 \text{ }^\circ\text{C}$

300 °C and 400 °C. The stress-strain curve at a strain rate of 0.1 s<sup>-1</sup> shows an upward trend in Figure 7. It indicates that the effect of work hardening is greater than that of dynamic softening. However, stress-strain value decreases with the increase of the strain after peak strain at higher strain rates of 1.0 s<sup>-1</sup> and 10.0 s<sup>-1</sup>. Dynamic softening takes place during compression at higher strain rates. There is an intersection of stress-strain curve for three different strain rates. The strain at the intersection point is defined as the critical strain. Figure 7 shows the critical strain is about 0.35, 0.29, 0.22 and 0.05, respectively, at 100 °C, 200 °C, 300 °C and 400 °C. It can be concluded that critical strain decreases with the increase of the deformation temperature. It indicates that the dynamic softening was enhanced with the increase of the deformation temperature for higher strain rates of 1.0 s<sup>-1</sup> and 10.0 s<sup>-1</sup> in the temperature range of 100 °C to 400 °C.

Before the critical strain, the true flow stress increases with the increase of the strain rates. After the critical strain, the true flow stress decreases with the increase of strain rates. According to the analysis of Section 3.2, the softening mechanism is predominant by microstructure spheroidization at lower deformation temperatures and higher strain rates.<sup>18</sup>

Figure 8 shows the stress-strain relationships of Ti-3Al-5Mo-4.5V at strain rates of 0.1 s<sup>-1</sup>, 1.0 s<sup>-1</sup> and 10.0 s<sup>-1</sup> with temperatures of 500 °C, 600 °C, 700 °C and

800 °C. The flow stress value decreases with the increase of true strain at a strain rate of 0.1 s<sup>-1</sup> when the temperature is higher than 500 °C. With the increase of deformation temperature, the stress decreases more obviously. It indicates that the dynamic softening was improved with the deformation temperature at a strain rate of 0.1 s<sup>-1</sup>. The detailed material softening mechanism at a strain rate of 0.1 s<sup>-1</sup> will be discussed in Section 3.5.

When the deformation temperature is higher than 600 °C, the variation law of flow stress conforms to the normal, i.e., the stress value of higher strain rate is greater than that at the lower strain rate. All stress-strain curves show a downward trend, which appears obvious dynamic material softening. According to Section 3.2, the transformation from a small amount of  $\alpha$  phase into  $\beta$  phase can be observed in Figure 6f. When the internal temperature of the specimen reaches the phase-transition temperature, some of the harder  $\alpha$  phase was transformed into softer  $\beta$  phase, which made the flow stress decline.<sup>19</sup>

### 3.4 Effect of deformation rates on microstructure evolution

Figure 9 shows SEM micrographs of Ti-3Al-5Mo-4.5V titanium alloy under true strain of 1.0 at 600 °C and strain rates of 0.1 s<sup>-1</sup>, 1.0 s<sup>-1</sup> and 10.0 s<sup>-1</sup>. Figure 10 shows the effect of strain rates on the volume

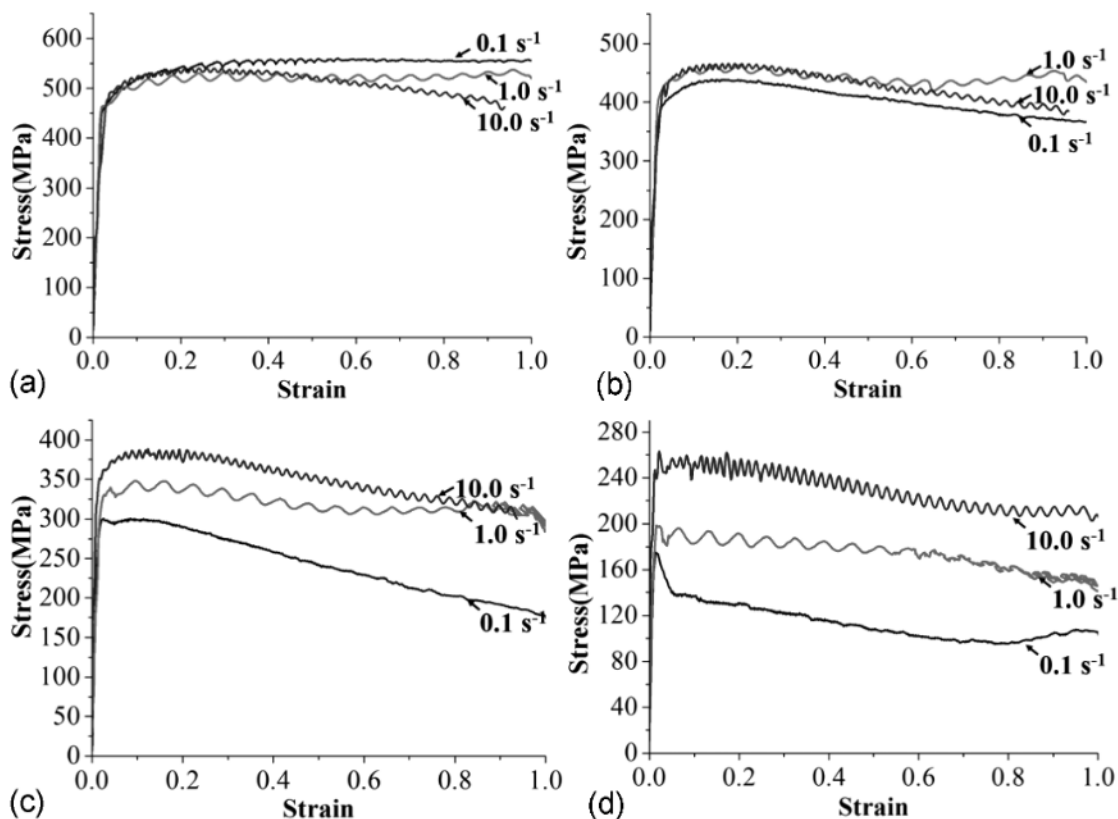


Figure 8: Stress-strain relationships of Ti-3Al-5Mo-4.5V at strain rates of 0.1, 1.0 and 10.0 s<sup>-1</sup> with temperatures of: a) 500 °C, b) 600 °C, c) 700 °C and d) 800 °C

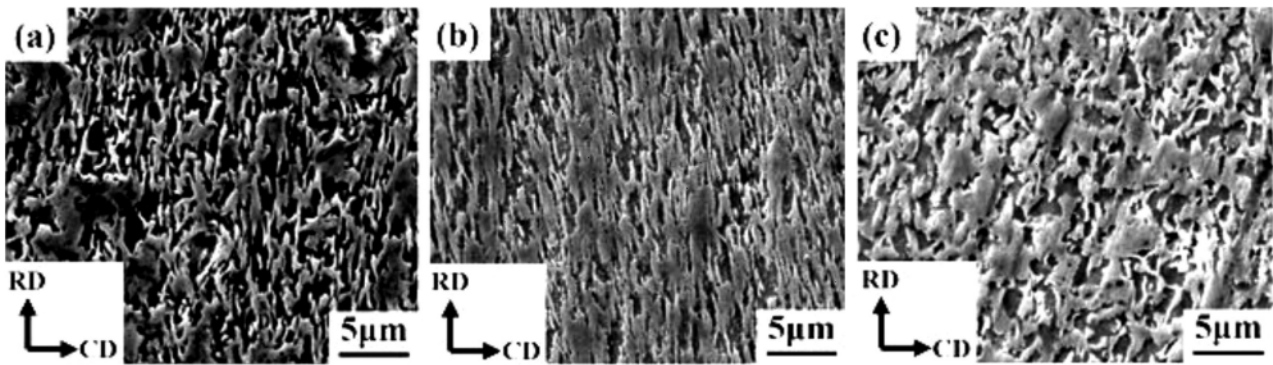


Figure 9: SEM micrographs of Ti-3Al-5Mo-4.5V under true strain of 1.0 at 600 °C and strain rates of: a) 0.1 s<sup>-1</sup>, b) 1.0 s<sup>-1</sup> and c) 10.0 s<sup>-1</sup>

fraction of  $\beta$  phase under true strain of 1.0 at 600 °C. The volume fraction of  $\beta$  phase is the area of all  $\beta$  phase divided by the total area of the image.<sup>20</sup> Under a lower strain rate of 0.1 s<sup>-1</sup>, the volume fraction of  $\beta$  phase is the smallest, i.e., 0.65, shown in Figure 9a. As the strain rate increases, the number of small-sized  $\alpha$  phase increases for a strain rate of 1.0 s<sup>-1</sup>, shown in Figure 9b. The volume fraction of  $\beta$  phase is 0.78 at a strain rate of 1.0 s<sup>-1</sup>. When the strain rate reached 10.0 s<sup>-1</sup>, the volume fraction of  $\beta$  phase is the largest. The volume fraction of  $\beta$  phase is about 0.81 at the strain rate of 10.0 s<sup>-1</sup>. Figure 9 and Figure 10 show that the volume fraction of  $\beta$  phase increases with the increase of the strain rates. This is because there is sufficient thermal activation energy when the strain rate is higher.<sup>21</sup> It is conducive to the transformation of  $\beta$  phase. So, the formation of  $\beta$  phase happens more easily at higher strain rates.

### 3.5 Softening mechanism analysis during hot compression

Figure 11 shows the SEM micrographs of Ti-3Al-5Mo-4.5V under a strain rate of 1.0 s<sup>-1</sup> and strain of 1.0 at 500 °C, 600 °C, 700 °C and 800 °C. It can be seen from Figure 11 that the phenomenon of microstructure coarsening becomes more obvious with the increase of the deformation temperature. This result can be attributed to the fact that the large deformation resistance

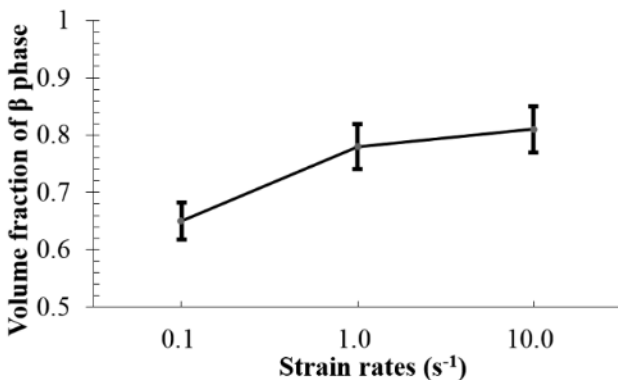


Figure 10: Effect of strain rates on the volume fraction of  $\beta$  phase under true strain of 1.0 at 600 °C

caused the local temperature rise, and then a small amount of  $\beta$  phase grows and forms coarse grains. Local temperature rise easily occurs within the microstructure of Ti-3Al-5Mo-4.5V. The stress-strain curves show a material-softening trend at temperatures of 500–800 °C under strain rate of 0.1 s<sup>-1</sup>, shown in Figure 8. The local temperature rise accelerates the movement of the dislocations, and it facilitates the processes of annihilation and climbing and then alleviates the work hardening.<sup>14</sup>

Therefore, local temperature rise causes material softening at lower strain rate of 0.1 s<sup>-1</sup> and higher deformation temperatures of 500–800 °C. From above analysis in Section 3.2, we know that the microstructure spheroidization is predominant for material softening at the higher strain rate of 10.0 s<sup>-1</sup> and the lower deformation temperatures of 100–400 °C.

## 4 CONCLUSIONS

The critical deformation temperature is 500 °C to distinguish the warm-deformation region of 100–400 °C and the hot-deformation region of 500–800 °C. Local

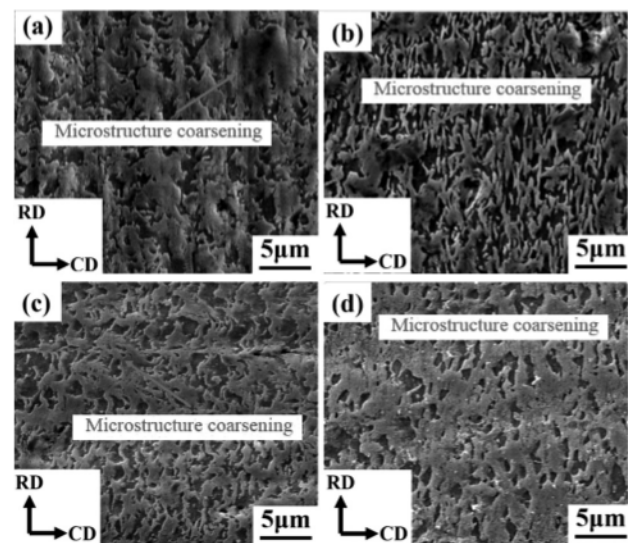


Figure 11: SEM micrographs of Ti-3Al-5Mo-4.5V under a strain rate of 0.1 s<sup>-1</sup> and strain of 1.0 at different temperatures of: a) 500 °C, b) 600 °C, c) 700 °C and d) 800 °C

temperature rise causes material softening at lower strain rate of  $0.1 \text{ s}^{-1}$  and higher deformation temperatures of  $500\text{--}800 \text{ }^\circ\text{C}$ . The microstructure spheroidization is predominant for material softening at the higher strain rate of  $10.0 \text{ s}^{-1}$  and the lower deformation temperatures of  $100\text{--}400 \text{ }^\circ\text{C}$ .

At deformation temperature of  $100\text{--}400 \text{ }^\circ\text{C}$ , there is an intersection point of the stress-strain curve for different strain rates, which is defined as critical strain. Before the critical strain, the true flow stress increases with the increase of the strain rates. After the critical strain, the true flow stress decreases with the increase of the strain rates. Critical strain decreases with an increase of the deformation temperature. It indicated that the dynamic softening was enhanced with the deformation temperature for higher strain rates of  $1.0 \text{ s}^{-1}$  and  $10.0 \text{ s}^{-1}$ .

The phase transition of the  $\alpha$  phase is obvious at the temperature range of  $700\text{--}800 \text{ }^\circ\text{C}$ . For the same strain rate, deformation temperature of  $400 \text{ }^\circ\text{C}$  is beneficial for manufacturing Ti-3Al-5Mo-4.5V with good mechanical properties and a uniform microstructure. At deformation temperature of  $600 \text{ }^\circ\text{C}$ , the volume fraction of  $\beta$  phase increases with the increase of strain rates.

## Acknowledgments

This project is funded by the National Natural Science Foundation of China (Grant No. 51805314), National Key Research and Development Program of China (Grant No. 2018YFB1307900), Shanghai Science and Technology Commission (Grant No. 16030501200).

## 5 REFERENCES

- P. Gao, Y. Cai, M. Zhan, X. Fan, Z. Lei, Crystallographic orientation evolution during the development of tri-modal microstructure in the hot working of TA15 titanium alloy, *Journal of Alloys & Compounds*, 741 (2018), 734–745, doi:10.1016/j.jallcom.2018.01.222
- S. Fujishiro, D. Eylon, T. Kishi, *Metallurgy and Technology of Practical Titanium Alloys*, TMS, 1994
- X. Zhao, Y. Qing, C. Bai, *Titanium Alloy and its Application*, Chemical Industry Press, Beijing, 2005
- B. F. Wang, Adiabatic shear band in a Ti-3Al-5Mo-4.5V Titanium alloy, *Journal of Materials Science*, 43 (2008), 1576–1582, doi:10.1007/s10853-007-2330-2
- X. W. Li, M. X. Lu, A. X. Sha, L. Zhang, The tensile deformation behavior of Ti-3Al-4.5V-5Mo titanium alloy, *Materials Science & Engineering A*, 490 (2008) 1–2, 193–197, doi:10.1016/j.msea.2008.01.086
- C. Wu, Effects of Heat Upset on Structure and Properties of TC16 Titanium Alloy, *Aerospace Materials & Technology*, 76 (2007) 3, 61–64, doi:10.3969/j.issn.1007-2330.2007.03.018
- H. Song, G. Q. Wu, Z. G. Zhang, Effects of microstructural variations on dynamic compressive deformation behavior of Ti-3Al-5Mo-5V alloy, *Materials Letters*, 60 (2006) 28, 3385–3389, doi:10.1016/j.matlet.2006.03.088
- W. Gao, Q. Fen, Z. Zhi, Microstructure Evolution in the Process of Hotworking the TC16 Titanium Alloy Bar, *Special Steel Technology*, 24 (2018) 2, 36–38, doi:10.16683/J.CNKI.ISSN1674-0971.2018.1026
- M. Shen, Y. Huo, T. He, Y. Xue, X. Jiang, Comparison of two constitutive modelling methods in application of TC16 alloy at the elevated deformation temperature, *Materials Today Communications*, 24 (2020), doi:10.1016/j.mtcomm.2020.101053
- S. Zharebtsov, M. Murzinova, G. Salishchev, S. L. Semiatin, Spheroidization of the lamellar microstructure in Ti-6Al-4V alloy during warm deformation and annealing, *Acta Materialia*, 59 (2011) 10, 4138–4150, doi:10.1016/j.actamat.2011.03.037
- B. R. W. G., *Materials Properties Handbook: Titanium Alloy*, ASM International, OH, Materials Park, 1994
- H. Zhang, G. Lin, D. Peng, L. Yang, Q. Lin, Dynamic and static softening behaviors of aluminum alloys during multistage hot deformation, *Journal of Materials Processing Technology*, 148 (2004) 2, 245–249, doi:10.1016/j.jmatprotec.2003.12.020
- R. Ding, Z. Guo, A. Wilson, Microstructural evolution of a Ti-6Al-4V alloy during thermomechanical processing, *Materials Science & Engineering A*, 327 (2002) 2, 233–245, doi:10.1016/S0921-5093(01)01531-3
- M. Li, H. Li, J. Luo, *Precision forging of titanium alloy*, Science Press, Beijing, 2016
- J. Luo, J. Gao, L. Li, M. Li, The flow behavior and the deformation mechanisms of Ti-6Al-2Zr-2Sn-2Mo-1.5Cr-2Nb alloy during isothermal compression, *Journal of Alloys and Compounds*, 667 (2016), 44–52, doi:10.1016/j.jallcom.2016.01.164
- J. Li, B. Wang, H. He, F. Shuang, J. Shen, Unified modelling of the flow behaviour and softening mechanism of a TC6 titanium alloy during hot deformation, *Journal of Alloys and Compounds*, 748 (2018), 1031–1043, doi:10.1016/j.jallcom.2018.03.120
- L. Li, M. Li, Evolution characterization of  $\alpha$  lamellae during isothermal compression of TC17 alloy with colony- $\alpha$  microstructure, *Materials Science & Engineering A*, 712 (2017), 637–644, doi:10.1016/j.msea.2017.12.023
- Z. Yuan, F. Li, H. Qiao, M. Xiao, J. Cai, J. Li, A modified constitutive equation for elevated temperature flow behavior of Ti-6Al-4V alloy based on double multiple nonlinear regression, *Materials Science & Engineering A*, 578 (2013), 260–270, doi:10.1016/j.msea.2013.04.091
- W. S. Lee, C. Y. Liu, The effects of temperature and strain rate on the dynamic flow behaviour of different steels, *Materials Science & Engineering A*, 426 (2006) 1–2, 101–113, doi:10.1016/j.msea.2006.03.087
- X. G. Fan, H. Yang, P. F. Gao, Prediction of constitutive behavior and microstructure evolution in hot deformation of TA15 titanium alloy, *Materials & Design*, 51 (2013), 34–42, doi:10.1016/j.matdes.2013.03.103
- Y. Huo, T. He, S. Chen, R. Wu, Mechanical Behavior and Microstructure Evolution of Bearing Steel 52100 During Warm Compression, *Jom*, 70 (2018), 1112–1117, doi:10.1007/s11837-018-2914-0